XVIII International Conference on Water Resources
CMWR 2010
J. Carrera (Ed)
CIMNE, Barcelona 2010

SIMULATION OF GRAVITY DOMINATED DNAPL INSTABILITIES IN SATURATED POROUS MEDUIM USING A PORE SCALE MODEL

K. NSIR, G. SCHÄFER

Laboratoire d'Hydrologie et de Géochimie de Strasbourg (LHyGeS)
UMR 7517, CNRS – Université de Strasbourg (UdS), 1 rue Blessig,
67084 STRASBOURG Cedex.
e-mail: nsir@unistra.fr, web page://www. lhyges.u-strasbg.fr

Key words: displacement, gravity instabilities, DNAPL, porous medium, network

Summary. *In this study we present a pore-scale network model to simulate gravity dominated displacement of a wetting fluid (water) by a lower-viscosity DNAPL (trichloroethylene) in homogenous porous media. A typical geometric representation of the network model includes a regular cubic lattice structure with pore bodies corresponding to the vertices of the lattice, and pore throats connecting the pore bodies. Both size distributions of the pores bodies and pores throats are determined by a probabilistic approach that computes the distribution of the volume of the voids in packed spheres. The model is used to simulate laboratory experiments conducted on a glass column having a length of 68 cm and 10 cm of diameter, filled with medium quartz sand. The calculated arrival times of the DNAPL front are compared with those measured using optic fiber probes placed at 8 points of the control section of the experimental device. Furthermore, the mean pressure of TCE measured during the experiment at the column inlet section was compared to the transient pressure predicted by the pore-throat-model. Globally, the numerical results obtained were in good agreement with the measurements.*

1 INTRODUCTION

Dense nonaqueous phase liquids (DNAPL) are immiscible with water and can give rise to highly fingered fluid distributions when infiltrating through water-saturated porous media. Generally two approaches are used to study the displacement process through porous media: the first is based on the continuum description of the porous medium associated with macroscpics laws such as Muskat's law to represent the volumetric flow vector for each fluid phase on the REV scale [1]; the second is based on the microscopic description of the pore geometry and on the physical laws of flow and transport within the pores [2, 3]. One of the common tools that have been used to do this is pore-scale network modelling, which requires a detailed understanding of the physical processes occurring at the pore scale. In the past, network models have been developed to study a wide range of single and multiphase flow processes, focusing on (i) the effect of pore structure on relative permeability for each fluid phase and on the hysteresis of capillary pressure curves in two phase systems [6], (ii) the functional relationship between capillary pressure, saturation and interfacial areas [11], and (iii) the behavior of the stable/unstable DNAPL front during drainage and imbibition [5,7,8,10,13]. Our work is dealing with the study of gravity-dominated displacement of

DNAPL in a homogenous water-saturated porous medium using a pore scale modeling approach. The model developed is an efficient tool to take into account the different forces and their competition affecting the occurrence of density-driven instabilities.

To get a predictive network model, the parameters used to generate both pore size distribution and throat size distribution are quantified using a grain-size distribution based geometrical model of an array of spheres combined with an approach of probability [12]. The results of simulation are then compared to a laboratory experiment conducted on a sand-filled column where the pressure at its entrance section during the displacement of TCE and the arrival time distribution of the DNAPL front in a cross-section were measured.

2 NETWORK MODEL

Pore-scale network models typically represent the pore space of the medium using simplified geometries, and within this geometric representation solve equations to track explicitly the location of all fluid–fluid interfaces within the network.

2.1 Pore space geometry

The pore network simulated in the model is a cubic lattice with constant node spacing. The pore bodies are represented by spheres. Similarly, pore throats are cylindrical with a circular cross-section (Figure 1).The location of water-DNAPL interfaces are restricted to the connection between the pore body and pore throat.

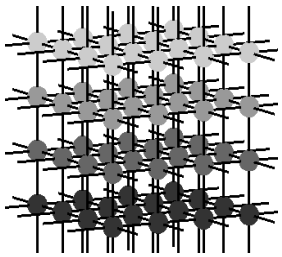

Figure 1: 3D view of a network

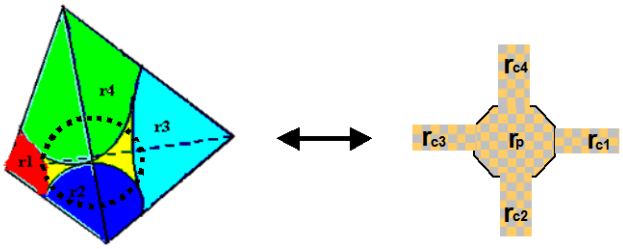

Figure 2: Schematic illustration of a tetrahedral subunit and its pore space approximation

The pore space is constructed by assigning radii to the lattice elements using a Weibull distribution [15] frequently used to develop network analogs of porous media. The statistic distribution is attractive due to its flexibility and the fact that it has fixed parameters which describe the characteristics of the size of pores and throats of the network. A minimum, average and maximum radius for both pore and throat are therefore required to define the pore-size distribution and throat-size distribution in the network. The probability distribution used is given by:

$$g(x) = \frac{x}{x_2^2}\exp\left(-\frac{x^2}{x_2^2}\right) \quad \text{for } x \leq x_3, \qquad = 0 \quad \text{for } x > x_3 \tag{1}$$

where $x = r - r_{min}$; $x2 = r_{moy} - r_{min}$, and $x3 = r_{max} - r_{min}$; r represents the pore-throat or body radius, r_{min} , r_{moy} and r_{max} are the minimum, average and maximum sizes, respectively. These typical parameters (r_{min}, r_{moy}, r_{max}) used for the construction of an equivalent network are evaluated by a model of an array of sphere packings coupled with an approach of probability.

A packing of spheres is supposed to be formed by groups of four touching spheres forming tetrahedral subunits (Figure 2). The pore space in a subunit has a narrow throat in each of the four faces of the subunit which meet at a central cavity. The size of a pore throat is evaluated by a cylinder with a diameter given by the in-sphere between the three spheres in the face. The pore cavity is determined by the in-sphere between the four touching spheres. Formulas for calculating pore body size and pore throat size and their relative probability density are available in [4, 12].

The array of sphere packings consists of a discrete particle size distribution (PSD) which is derived from the grain-size distribution of the porous media. From the obtained PSD we extracted equally spaced sphere radii, for which we calculated the corresponding density probability. For each set of four radii, we computed the probability of the tetrahedron submits and the corresponding radius of the 'kissing' sphere. The final result was a one pore size distribution curve and four throat size distribution curves [9]. A statistical analysis of these distributions allowed us in a second step to calculate various ranges of radii of pore body and pore throat.

2.2 Governing flow equations of the pore-throat model

The developed network model uses the following assumptions [10]: (i) fluids used are Newtonian, incompressible and immiscible; (ii) the flow is laminar; (iii) the local capillary pressure in the pore bodies is negligible, resulting in only one mean pressure within a pore body, independent of the phase saturation of that pore body; (iv) the volume of the pore throats is small compared to the overall volume of pore bodies.

The mass balance equation for each pore can then be written as follows

$$\sum_j q_{ij} = Q_i^e \tag{2}$$

where q_{ij} denotes the flow rate through a throat connecting porenode i and and pore j. Q_i^e is the external flow rate into pore i, which is zero unless the pore is located at flow boundary. The sum runs over all neighboring pores of pore i. The expression that has to be used for the flow rate q_{ij} depends both on the fluid present in the pore throat connecting pores i and j and on the presence of a meniscus within the pore throat.

If no meniscus is present in the pore throat, the flow rate q_{ij} through the pore throat is given by Poiseuille's Law

$$Q_{ij} = \frac{\pi r_{ij}^4}{8\mu_\alpha}(P_i - P_j - (z_i - z_j)\rho_\alpha g) \tag{3}$$

If a meniscus is present, the flow rate q_{ij} through the pore throat is given by the Washburn

equation [15].

$$Q_{ij} = \chi\left\langle P_i - P_j - (z_i - z_j)\rho_\alpha g - P_c(r_{ij})\right\rangle \frac{\pi r_{ij}^4}{8\bar{\mu}}(P_i - P_j - (z_i - z_j)\bar{\rho}g - P_c(r_{ij})) \quad (4)$$

We introduced in equation (4) ‘‘effective’’ viscosities and densities for μ_{ij} and ρ_{ij} , which are defined by

$$\bar{\mu} = \mu_{nw}S_{ij} + (1 - S_{ij})\mu_w \quad (5)$$

$$\bar{\rho} = \rho_{nw}(S_{ij}) + (1 - S_{ij})\rho_w$$

$$S_{ij} = (S_i + S_j)/2\cdot$$

S_{ij} is an average saturation between pore i et j. $Pc(r_{ij})$ used in equation (4) denotes the capillary entry pressure assigned to throat (ij) which needs to be exceeded by the DNAPL to enter the water filled throat. Its expression is given by Young Laplace’s Law

$$P_c(r_{ij}) = \frac{2\sigma\cos\theta}{r_{ij}} \quad (6)$$

where θ is the contact angle (assumed to be 0) and r_{ij} is the radius of the pore throat connecting pore i and pore j.

χ <X> appearing in Eq. 4 is a Heaviside function that stands for the displacement condition of the interface in pore throat. The throat can be blocked by capillarity if the capillary entry pressure ($Pc(r_{ij})$) was not yet reached. The Heaviside function is defined by

$$\chi\langle X\rangle = \begin{cases} 1, & \text{for } X \succ 0 \\ 0, & \text{for } X \leq 0 \end{cases} \quad (7)$$

Using the appropriate expression of flow rate q_{ij} in Eq.(2) provides a set of algebraic equations with the pore-body pressures as unknowns. This set of equation can be written in matrix form as follows:

$$D\,P = B \quad (8)$$

where D is the conductance matrix whose elements depend on the connection between different throats. P denotes the pressure vector. Vector B contains the pressure and the flow rate at the boundaries and the capillary pressure if a meniscus is present in the throat. The matrix system is solved using implicit time scheme in pressure and explicit time scheme for saturation terms [13]

3 NUMERICAL RESULTS AND DISCUSSION

3.1 Model parameters

One of the objectives of our study was to use experimental results [9] for verification of the

developed network model. Experiments were conducted in a sand-filled glass column with a length of 68 cm and inner diameter of 10 cm. The DNAPL used was trichloroethylene (TCE) injected at a constant flow rate of 40 mL/min. The displacement was performed from up to down, unstable gravity condition, and down to up, stable displacement condition. The experimental device was equipped with pressure transducers for monitoring pressure at the inlet and outlet section of the glass column. The experimental program allowed also a measurement of the arrival time of the DNAPL front at eight points of a control section equipped with fiber optic probes [9].

Simulations reported here were carried out on a network of 5×5×4858, 7×7×4858 and 9×9×4858 pore bodies. The spatial discretisation used reproduces the total height of the physical model but only a small fraction of the column section. We assumed that the chosen network is sufficiently large to get a statistically homogeneous network which may be representative to reproduce the macroscopic properties of the sand column such as intrinsic permeability and porosity. The parameters for pore body and pore throat radii derived from the packing sphere model using the grain-size distribution of the porous medium are given in Table 1 [9].

Distance between pore body centre (L)	0.14 [mm]
Pore body mean (r_{moy})	0.048 [mm]
Pore body minimum (r_{min})	0.042 [mm]
Pore body maximum (r_{max})	0.057 [mm]
Pore throat mean (r_{moy})	0.017 [mm]
Pore throat minimum (r_{min})	0.030 [mm]
Pore throat maximum (r_{max})	0.036 [mm]

Table 1: Distribution parameters for pore and throat radius

The network was initially water saturated ; a constant flow rate of 40 mL/min of water respectively TCE was applied at the inlet section of the model. At the outlet face the observed water head was specified as constant pressure boundary. The numerical solution of the flow equations (Eq.8) provides inlet pressure values for each time step. Furthermore, the arrival times of the TCE front at a cross section of the network were calculated. Numerical results are compared to the measurements.

3.2 Stable case of water displacement by DNAPL

To illustrate the case of stable displacement, the displacing fluid (DNAPL) is injected at the bottom of the network. The injection rate was calculated taking into account the section modeled in relation to the total section of the experiment. Therefore we used a TCE injection rate of 5.28×10^{-5}, 6.06×10^{-5} and 6.06×10^{-5} $mLmin^{-1}$ respectively for the networks of 5×5×4858, 7×7×4858 and 9×9×4858 pore bodies. The boundary pressure applied to the outlet section corresponded to a water height of 18 cm. The simulation stopped when the equivalent volume of DNAPL used in the experiment was injected.

Figure 3 shows the comparison of calculated and measured inlet pressure as function of

time. Accordingly to the experimental observation, the pressure field increases with time. The DNAPL/water front is stabilized by the gravity effect; the possibly destabilizing influence of the viscosity ratio on the front behavior is not significant. Furthermore, the simulated pressures for the different network discretisations are quite similar. Due to the stabilizing gravity effect, a flat piston-like front is obtained moving through the network. Consequently, very little wetting fluid is left behind and a compact pattern of the invading fluid takes place. The increase of the pressure is caused by the high density of the invading fluid which overrides the decrease of viscous pressure during the displacement of the less viscous DNAPL. The numerical tool reproduces the behavior of pressure increase observed in the experiment. However, we note that the measured pressure increases more strongly than that calculated. This can be explained by the chosen arrangement of the pore and throat size in the pore-throat model. Very narrow capillaries existing in the real porous medium and not considered in the network may require a higher displacement pressure in order to be invaded by the displacing fluid.

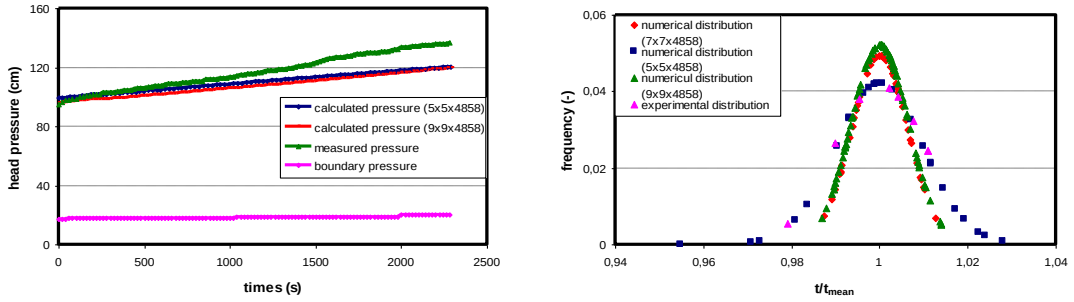

(a) (b)

Figure 3: Stable displacement of water by DNAPL: (a) inlet pressure measured and simulated as function of time and (b) distribution of calculated and measured dimensionless arrival times of the DNAPL front

The curves representing the distributions of arrival times of the DNAPL front measured and calculated (Figure 3 (b)) are in good agreement. The standard deviation calculated for the network pore discretization of 5×5×4858 is very close to that measured. We note a value of 8 s for the small network compared to 9 s measured in the experiment. According to our experimental observations, the distribution of front arrival times at the cross section is almost uniform. The model reproduces adequately the stability mechanisms of displacement caused by the positive contribution of gravity.

3.2 Unstable case of water displacement by DNAPL

In this case, the DNAPL is injected at the top of the network using the same boundary and initial conditions as described in section 3.1. For this type of displacement, we expect a much more irregular front with possible gravity fingering. Figure 4 shows the variation of displacement pressure mesured and calculated by the model.

Due to the constant injection rate, the pressure field decreases as the less viscous and denser fluid invades the system. The inlet pressure observed is well reproduced by the

numerical model. Nevertheless, the rate of which it decreases is different from the one measured. The calculated decrease of pressure is higher than the one observed.

Under these displacement conditions, gravity forces are destabilizing and dominate the movement resulting in typical DNAPL fingers into the defending fluid. The macrosopic interface water / TCE is not anymore horizontal and many throats may be blocked by the capillary effect. The number of active paths of invasion is therefore low and the flow section of TEC is reduced. The contribution of viscous pressure is also limited and dominated by the contribution of the higher density of the invading fluid resulting in a decrease of the inlet pressure. Therefore, the overall inlet pressure decreases with time. The sudden increase of the pressure as shown in Figure 4 corresponds to the breakthrough of the invading fluid at the outlet section. In our numerical simulations we recorded the time of breakthrough earlier than that observed, especially in the case of high numbers of pore bodies used. One can explain this result by the number of active paths of invasion which is apparently lower in the network model than in the real porous medium.

Gravity fingering is numerically confirmed by the distribution of arrival times of the front at the chosen cross section of the network. Figure 4 shows the comparison of the distribution of arrival times of the front calculated and observed at the control section. The statistical analysis of the distribution of arrival times of the front illustrates a highly non-uniform distribution of arrival times with a significant standard deviation.

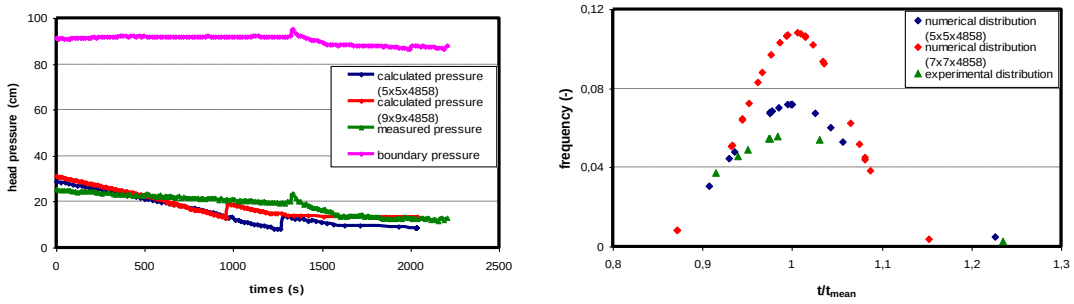

(a) (b)

Figure 4: Unstable displacement of water by DNAPL: (a) inlet pressure measured and simulated as function of time and (b) distribution of calculated and measured arrival times of the DNAPL front..

4 CONCLUSIONS

In summary, we developed a simulator that describes the dynamic drainage process. The model of paching sphere combined with a probability approach is used to obtain realistic pore-sizes and throat-sizes based on a grain-size distribution. The implementation of the pore-scale network model was tested using experimental data. The prediction of both the temporal evolution of pressure at the inlet section and the distribution of arrival times of the front in a given cross section were in good agreement with laboratory measurements. An important feature of the model is its capability to reproduce the observed pressure behaviour for stable and unstable displacement regimes. Accordingly to the laboratory experiment, the pressure at the inlet section increases with time in the case of a stable water displacement. However, in

the case of unstable displacement, the pressure decreases due to the occurrence of gravity DNAPL fingering. Further research work might focus on a sensitivity study of the influence of the chosen minimum, mean and maximum size of pore bodies and pore throats on the measured variables such as transient pressure and arrival times of the displacement front.

ACKNOWLEDGEMENT

Financial support for this research from the program REseau Alsace de Laboratoires en Ingénierie et Sciences pour l'Environnement (REALISE), the Région Alsace, the GDR «Hydrodynamique et Transferts dans les Hydrosystèmes Souterrains » (INSU-CNRS),

REFERENCES

[1] J. Bear. Dynamics of Fluids in Porous Media, Elsevier, New York, (1972).
[2] M Blunt and P. King. Macroscopic parameters from simulations of pore scale flow. Physical Review A, 42 (8), 4780-4787 (1990).
[3] M. A. Celia, P. C. Reeves and L. A. Ferrand. Recent advances in pore scale models for multiphase flow in porous media. Reviews of Geophysics, 33(2), 1049-1058 (1995).
[4] J. A. Dodds. The Properties of Multicomponent Sphere Packings by a Simple Statistical Geometric Model, J. Colloid and Interface Sci., 77, 317–327 (1980).
[5] M. Hilpert, and C. T. Miller. Pore-morphology-based simulation of drainage in totally wetting porous media, Advances in Water Resources, 24, 243-255 (2001).
[6] G. R. Jeraul, and S. J. Salter. The effect of pore-structure on hysteresis in relative permeability and capillary pressure: pore level modeling. Transport in Porous Media, 5, 103-151 (1990).
[7] M. I. Lowry and C. T. Miller. Pore-scale modeling of nonwetting-phase residual in porous media. Water Resources Research, 31(3), 455-473 (1995).
[8] H.F. Nordhaug, M. Celia and H.K. Dahle. A pore network model for calculation of interfacial velocities, Advances in Water Resources, 26, 1061-1074 (2003)
[9] K. Nsir. Etude expérimentale et numérique de la migration des polluants non miscibles à l'échelle de Darcy. PhD thesis, Université de Strasbourg, France (2009).
[10] T.W Patzek. Verification of a complete pore network simulator of drainage and imbibition. Society of petroleum Engineers, 1-12 (2000).
[11] P.C. Reeves and M. A. Celia. A functional Relationship between capillary pressure, saturation, and interfacial areas as revealed by a pore-scale network model. Water Resources Research, 32(8), 2345-2358 (1996).
[12] Y.Rouault, S Assouline. A probabilistic approach towards modeling the relationships between particle and pore size distributions: the multicomponent packed sphere case. Powder Technology, 96, 33-41 (1998).
[13] M. Singh and K. Mohenty. Dynamic network for drainage through three dimensional porous materials, Chemical Engineering Science, 58, 1-18 (2003).
[14] E.W. Washburn. The dynamics of capillary flow. Phys. Rev., 17273 (1921).
[15] W. Weibull. A statistical distribution function of wide applicability. J. Appl. Mech., 18, 293-307 (1951).